In Situ Crosslinkable Gelatin Hydrogels For Vasculogenic Delivery of Mesenchymal Stem Cells

By

Sue Hyun Lee

Thesis

Submitted to the Faculty of the

Graduate School of Vanderbilt University

In partial fulfillment of the requirements

for the degree of

MASTER OF SCIENCE

In

Biomedical Engineering

December, 2013

Nashville, Tennessee

Approved:

Hak-Joon Sung, Ph.D.

Pampee P. Young, M.D. Ph.D

ACKNOWLEDGEMENTS

Foremost, I would like to thank my advisor, Dr. Hak-Joon Sung for his guidance and support, and countless learning opportunities he provided me with in so many ways for the past two very intense years. I also thank Dr. Pampee Young for her collaborative work and providing me with insight and suggestions in this work, as well as Dr. Ki Dong Park and his lab members who so willingly shared and encouraged further research with the material. Additionally, I acknowledge Dr. Young Wook Chun and Desirae Deskins who directly helped and performed many of the experiments. My undergraduate research assistants Jessica Kim, Frank Schumacher, and Anna Hwang have been essential in completing this work. I also owe it to the senior members of our lab, Spencer Crowder, Angela Zachman and Dr. Mukesh Gupta for both their tremendous mental support and technical insight, as I would not be here today without them. I also thank my fellow lab mates, Rutwik Rath, Timothy Boire, Daniel Balikov and Lucas Hofmeister for the friendship and kindly introducing me to their areas of work. Lastly, I would like to acknowledge my family who has always been unwaveringly supportive in all I do, and for all the great opportunities I've had in my life.

TABLE OF CONTENTS

LIST OF TABLES

LIST OF FIGURES

Figure Page

CHAPTER I

INTRODUCTION

Vasculogenesis and angiogenesis in tissue engineering

Vasculogenesis is a *de novo* formation of blood vessels while angiogenesis describes a process of new blood vessel formation from pre-existing vessels [1]. These processes enable vascularization of nearly all tissues in our body, with the notable exception of avascular cartilages, and this otherwise ubiquitous blood vessel network in tissues serves as an efficient transport system for distributing oxygen, nutrients and wastes to appropriate places. Passive diffusion of molecules alone is not sufficient for any substantial tissues exceeding ~200μm in thickness, and without thorough vascularization, necrosis takes place [2]. Hence, it is of paramount importance that any tissue engineering application includes careful considerations to strategies to either 1) vascularize the engineered construct prior to implantation or 2) design the constructs with careful choices on important parameters such as material compositions (haemocompatibility, soluble growth factors etc) and physical properties (ie. porosity) that will allow timely angiogenesis after implantation [3]. Unfortunately, vascularization in tissue engineering is still an outstanding challenge. Therefore, materials that readily induce angiogenesis and/or vasculogenesis *in vitro* and *in vivo* are sought-after and will bring tissue and organ engineering one step closer to reality.

Gelatin as a biomaterial

Gelatin is an irreversibly denatured and hydrolyzed form of collagen, which is the most abundant protein in our body that makes up the majority of the extracellular matrix. As such, gelatin is known for its excellent biocompatibility, biodegradability, adhesiveness, and non-immuno/antigenicity, in addition to the easy access and economic production when compared to

collagen [4]. Therefore, gelatin possesses numerous desirable characteristics for biological applications, and indeed it has been widely used as a preferred coating material for tissue culture plates, especially for primary endothelial cells that are especially difficult to culture *in vitro* [5]. However, the use of gelatin for tissue engineering application has been limited thus far mainly due to its low upper critical solution temperature below 35°C, which makes it impossible to engineer a thermo-stable gelatin construct for *in vivo* applications [6]. Accordingly, gelatin has been typically used as a component in composite materials, and there are very few studies employing purely gelatin-based materials. Because of this limited use, understanding of gelatin as a biomaterial remains shallow. Therefore, we have developed and characterized modified gelatin by conjugating hydroxyphenyl propionic acids to the gelatin backbone, which allows for *in situ* crosslinking upon reaction with H_2O_2 and horseradish peroxidase [7]. This design allows the fabrication of purely gelatin-based hydrogels that are injectable and thermo-stable. Its unknown biological effects and interactions with cells towards angiogenesis and vasculogenesis are the central topic of this study.

Mesenchymal stem cells in tissue engineering

Mesenchymal stem cells (MSCs) are a subset of non-hematopoeitic stem cells found in the bone marrow stroma, hence are also available in adults [8]. Since its discovery in the 1980s, MSCs have been one of the most intensely studied type of stem cells as a promising cell source in tissue engineering. Previous studies revealed the multipotent differentiative capacity of MSCs ranging from well-established differentiation into osteocytes, chondrocytes and adipocytes to more recently observed differentiation into various muscle cells, endothelial cells, and neurons (**Figure A**) [8 9]. It was also shown that not only did MSCs differentiate down diverse lineages, they also came with a few other desirable traits such as immunomodulation, and "drugstore"-like trophic activities that aid in regeneration [10]. Hence, we chose MSCs as a cell source for its multipotent nature as well as its

regenerative properties to investigate their biological effects and interactions with *in situ* crosslinkable gelatin material.

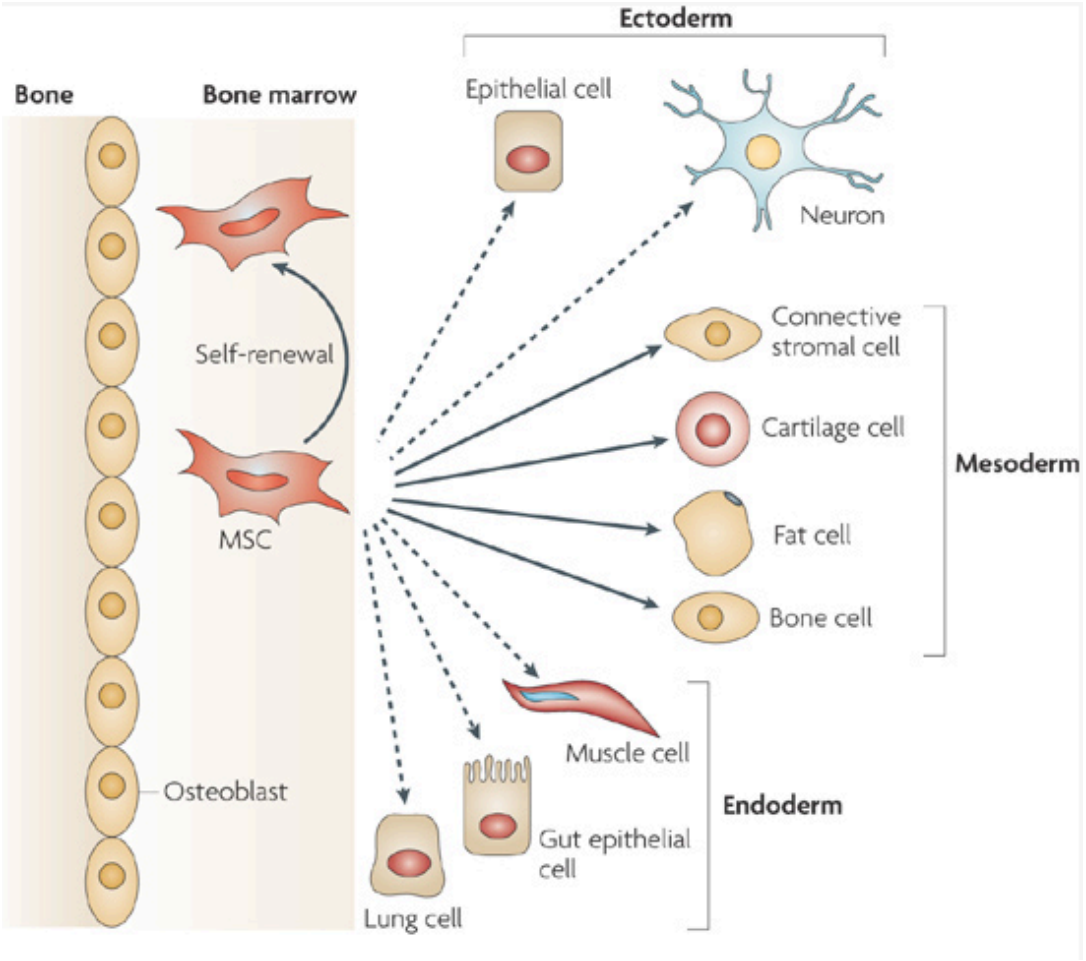

Figure A. This figure shows the ability of mesenchymal stem cells (MSCs) in the bone-marrow cavity to self-renew (curved arrow) and to differentiate (straight, solid arrows) towards the mesodermal lineage. The reported ability to transdifferentitiate into cells of other lineages (ectoderm and endoderm) is shown by dashed arrows, as transdifferentiation in controversial in vivo [9].

CHAPTER II

In Situ CROSSLINKABLE GELATIN HYDROGELS FOR ANGIOGENIC AND VASCULOGENIC DELIVERY OF MESENCHYMAL STEM CELLS

Motivation

In situ crosslinkable gelatin have been recently developed as a form of injectable hydrogel [7]. As this is one of the first studies employing purely gelatin-based 3D constructs, we initially aimed to characterize the basic biological properties of this material: for example, mesenchymal stem cell viability and their morphology in 3D encapsulation culture. Our initial investigation showed promising results in viability. However, we were most intrigued by the changes in MSC morphology and organization in these gelatin-based hydrogels over time. Soon we discovered that MSCs were differentiating towards an endothelial lineage *in vitro*, and the rest of the experiments in this study were designed to characterize the pro-vasculo/angiogenic effects of this gelatin material *in vitro* and *in vivo*.

Methods

Synthesis of Gelatin-Hydroxyphenyl Propionic Acid (GHPA)

Synthesis of GHPA has been described previously [7]. Briefly, hydroxyphenyl propionic acid (HPA) was first activated with 1-ethyl-3-(3-dimethylaminopropyl)-carbodiimide (EDC), N-hydroxysuccinimide (NHS) in a co-solvent of water and DMF (volume ratio of 3: 2). The activated HPA solution was then added to the pre-heated gelatin solution and stirred at 40°C for 24 hours. The resulting solution was transferred into a dialysis bag (MWCO. 3.5 kDa), dialyzed against deionized water for 3 days, filtered, and lyophilized to obtain the GHPA conjugates (**Figure 1A**).

Characterization of Elastic/Storage Moduli (G') of GHPA

GHPA was dissolved in DMEM media (Invitrogen) at 3-7% (wt) and divided into two aliquots; one was mixed with horseradish peroxidase (HRP, Sigma) at the final concentration of 2.5μg/ml, while the other aliquot was mixed with H_2O_2 (Sigma) at the final concentrations of 0.0025-0.01% (w/v). Solutions can be loaded onto separate syringes, and a dual-syringe applicator is used to evenly eject the two solutions, ensuring proper mixing and gelling (**Figure 1B**). Storage moduli (G') was measured in a parallel plate setting on a TA Instrument RA2000 rheometer in oscillation mode with a frequency of 1 Hz and 0.1% strain at 37°C.

***In Vitro* 3D Culture of Mesenchymal Stem Cells (MSCs) in GHPA**

Wild type murine mesenchymal stem cells (MSCs, GIBCO) from passage 12-14 or *Flk-1-LacZ* transgenic murine MSCs were used. GHPA and H_2O_2 were dissolved in DMEM media at various % (w/v) as indicated, while a constant concentration of 2.5μg/ml HRP was used in all conditions. Cells were added to the GHPA+HRP solution at the final concentration of 10^6 cells/ml. The same number of cells was seeded on tissue culture plate without GHPA gel to serve as a control. After GHPA gelled on the well plate, DMEM supplemented with 10% FBS (Invitrogen) and 1% penicillin-streptomycin (Invitrogen) was added and media was changed every day over 15 days.

Cell viability assay: cell viability was measured at days 1, 7, and 15 post culture using 5μM resazurin (Sigma). After 4 hours incubation of resazurin with cells, test culture media were transferred to a new 96-well plate for fluorescence readout at 590nm using a TECAN M1000 plate reader. On the same days, cells were also incubated in media containing 1μM calcein AM (Invitrogen) and 1μg/ml propidium iodide (Sigma) for 15 minutes then imaged by a Zeiss 710 confocal laser scanning microscope for identification of live/dead cells . Images were then z-stacked using ImageJ (NIH) for presentation.

MSC Delivery in GHPA Gels on Polyvinyl Alcohol (PVA) Scaffolds *In Vivo*

Subcutaneous implantation: *Flk-1-LacZ* transgenic murine MSCs were generously provided by Dr. Young lab as the expression of Flk-1, a VEGFR-2 receptor in MSCs can be detected *in situ* by staining LacZ to verify their endothelial differentiation *in vivo*. GHPA and H_2O_2 were dissolved in DMEM media at various % (w/v) as described above, while a constant concentration of 2.5μg/ml HRP was used in all conditions. Flk1-LacZ MSC ($5x10^5$)-containing GHPA gel solutions in total volume of 60μl were loaded on porous PVA scaffolds. The gel-scaffold complexes were then subcutaneously implanted on the ventral side of C57/bl6 mice for 2 weeks (**Figure 5A**). As a control, porous PVA scaffolds loaded with non-crosslinked GHPA gel solution containing Flk1-LacZ MSCs were implanted.

Characterization of implanted scaffolds: At 2 weeks, mice were perfused under heavy, near lethal level of anesthesia. First, they were perfused with PBS containing 0.1mg/ml heparin sulfate, followed by fluorescent microbeads (Invitrogen) for fluorescent micro-angiography. Scaffolds were subsequently harvested and analyzed for mRNA expression by RT-PCR, β-galactosidase activity by x-gal staining, angiogenesis by micro-angiography and CD31 staining, and the presence of remaining GHPA gel and general histological analysis by trichrome staining. Animal procedures were pre-approved by and performed in accordance with Vanderbilt IACUC.

Gene Expression Analysis via Quantitative Polymerase Chain Reaction (qRT-PCR)

Samples were homogenized in Trizol (Invitrogen), and RNA was collected using Rneasy kit (Qiagen). RNA concentration and 260/280 ratios were measured on a TECAN M1000 plate reader. RNA was treated with DNAse to eliminate genomic contamination, and reverse-transcribed using High Capacity cDNA Synthesis Kit (ABiosystems). SYBR Green PCR mix (Biorad) was used for quantitative PCR. Each sample containing at least 40 ng cDNA and 500nM of each primer with

annealing temperature at 55°C was run in technical triplicates, followed by melting curve analysis. Raw data were analyzed using CFX Manager (Biorad), and biological replicates from different animals were combined [11]. GAPDH expression was used for normalization, where the GAPDH expression level divides each gene expression level, and this number is set to 1 for the control. Primers used in this study are listed in **Table 1**.

Histological/Immunohistochemical Staining

Tissue preparation: Samples were fixed in 4% paraformaldehyde (PFA) for 24 hours at 4°C, washed with PBS, and immersed in 5%-30% sucrose solution until samples sank. Samples were then embedded in optimal cutting temperature (TissueTek) compound and frozen in acetone and dry ice bath. 15μm-thick slices were obtained by cryosectioning.

Trichrome green staining: General histology and trichrome green staining for the left over parts of GHPA gels in the sections were performed by Vanderbilt Research Histology Core.

β-galactosidase staining: Sample sections as well as positive and negative controls were fixed with 4% PFA for 10 min at room temperature, washed with PBS, and incubated at 37°C for 2 days in a solution containing the following: 27mM NaH_2PO_4, 73mM Na_2HPO_4, 2mM $MgCl_2$, 2mM EGTA, 1μg/ml NP40, 5mM $K_4[Fe(CN)_6]$, 5mM $K_3[Fe(CN)_6]$, and 1mg/ml x-gal (all chemicals from Sigma). Slides were then washed with dH_2O and mounted.

CD31 staining: Sample sections as well as a positive control was fixed with 4% PFA for 10 min at room temperature; washed with PBS, blocked with 10% goat serum and 1% bovine serum albumin overnight at 4°C; washed with PBS; and incubated with goat anti-mouse CD31 antibody (eBioscience) overnight at 4°C, followed by incubation with Dylight594-conjugated anti-goat IgG (Jackson Lab). Sections were then counter-stained with DAPI and mounted for imaging.

Imaging: Bright-field microscopy for β-galactosidase and trichrome green stain was performed on a Nikon Eclipse Ti scope, and fluorescence images for CD31 and micro-angiography

were acquired using a Zeiss 710 confocal laser microscope. ImageJ was used for z-stacking fluorescence images.

Statistical Analysis

Results are presented as means ± standard deviation (SD) or standard error mean (SEM) as indicated. Comparisons among different conditions were performed using an unpaired Student's t-test. For all statistics, $p < 0.05$ was considered statistically significant, and such significance is indicated where appropriate.

Results

Synthesis and Characterization of Gelatin-Hydroxyphenyl Propionic Acid (GHPA)

Hydrogels were successfully produced from hydroxyphenyl propionic acid-conjugated gelatin that underwent *in situ* oxidative crosslinking among the phenolic moieties catalyzed by H_2O_2 and HRP (**Figure 1**). As seen in **Figure 1B,** two GHPA solutions are prepared in order to avoid premature gelation where one GHPA solution contains HRP while the other GHPA contains H_2O_2. HRP or H_2O_2-containing GHPA solutions are loaded in separate syringes, and the solutions can be injected or sprayed for *in situ* cross-linking for various applications[7]. For cell experiments, cells were suspended in HRP-containing GHPA in order to minimize cytotoxicity due to H_2O_2 exposure.

Mechanical properties were characterized without cells at 37°C. All test materials underwent gelation within 20 seconds. The results from measuring storage moduli (G') of GHPA gels with varying GHPA and H_2O_2 concentrations are shown in **Figure 2**. Overall, crosslinked GHPA gels exhibited storage moduli ranging from ~100 Pa to ~2500 Pa which are typical of soft hydrogels.

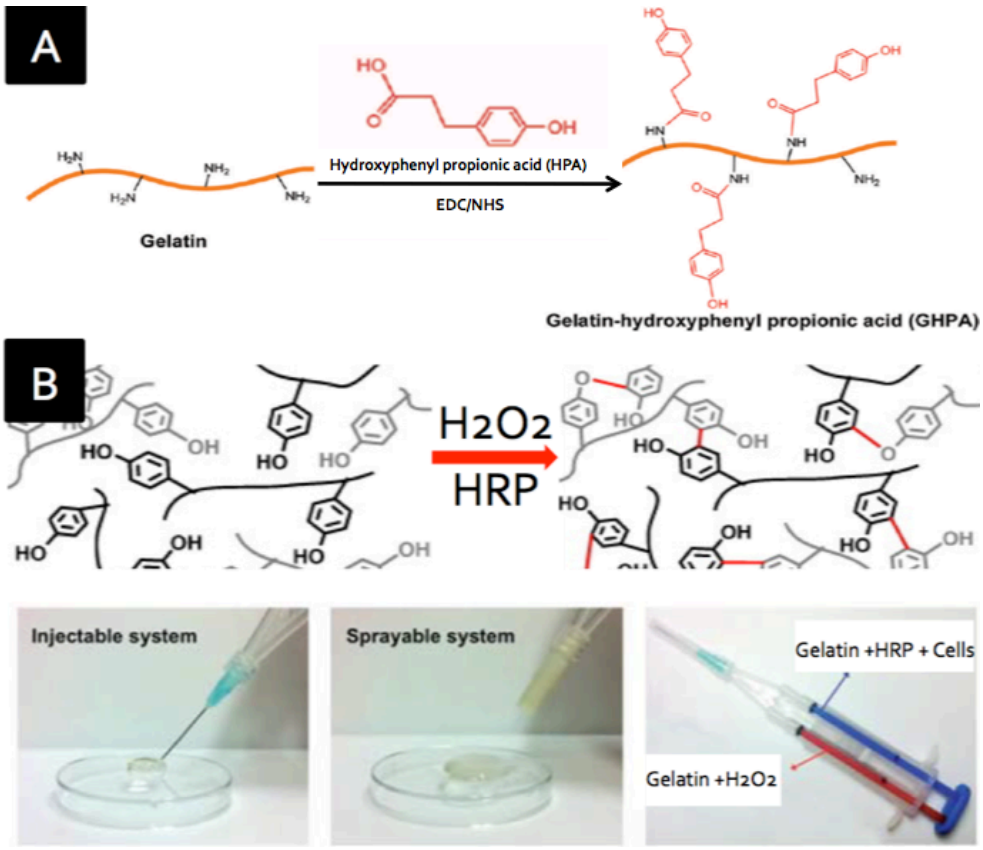

Figure 1. (A) Synthesis of gelatin-hydroxyphenyl propionic acid (GHPA). **(B)** Rapid gelation of GHPA by H_2O_2 and horseradish peroxidase (HRP)-catalyzed oxidative crosslinking. Bottom right image shows a dual-syringe system for cell-containing GHPA injections for *in situ* crosslinking, and this system can be used for injection or spraying.

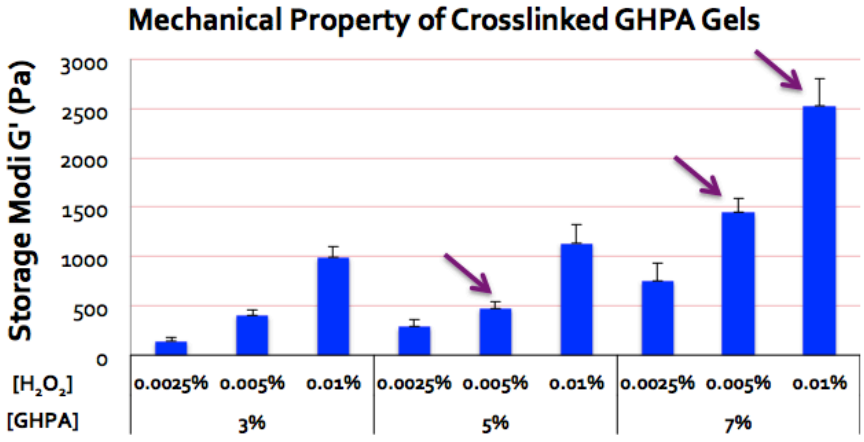

Figure 2. Storage moduli (G') of crosslinked GHPA gels with varying concentrations of GHPA [%w/v] and H_2O_2 [%w/v] were measured using a rheometer with N=3 and error bars = ±1 SEM. The compositions indicated with arrows were used for the following biological experiments.

An increase in either gelatin or hydrogen peroxide concentration resulted in an increase in the storage modulus as expected. Maximum GHPA concentration used was at 7% (w/v) due to the high viscosity. We chose to perform biological experiments with the three different formulations indicated with arrows in **Figure 2**. We mostly chose formulations with high moduli as hydrogels with high moduli have better hydrogel stability *in vivo.*

In Vitro 3D Culture of Mesenchymal Stem Cells (MSCs) in GHPA

Using the aforementioned dual-syringe system (**Figure 1B**), GHPA solutions containing MSCs, HRP, and H_2O_2 were mixed upon injection and gelled in a 24 well plate of tissue culture polystyrene (**TCPS**) for *in vitro* 3D culture over 15 days. Reduction of resazurin was used as an indicator of live metabolic cells, and it was measured on days 1, 7, and 15. The same number of MSCs cultured on TCPS without GHPA served as a control for 100% cell viability (**Figure 3A**). Among the different GHPA compositions there was no statistically difference in cell viability, although the condition with the highest GHPA and H_2O_2 contents (7%:0.01%) appeared to slightly lag behind the others. The higher concentration of hydrogen peroxide, a known cytotoxic agent, may account for the lower cell viability of 7%:0.01% condition. Similarly, initial MSC exposure to the remaining unreacted H_2O_2 could be responsible for the initially low cell viability for all GHPA conditions. Additionally, cell viability of MSCs in GHPA gels may have been limited by slow diffusion of nutrients and wastes through the crosslinked gelatin network, especially in a static culture condition. Despite its shortcomings, viability of MSCs in GHPA gels greatly improved to above 70% for all GHPA conditions on day 15 after a poor initial survival rate of ~20%.

Continuous improvement in cell viability of MSCs upon 3D GHPA culture over time was also evident in live/dead imaging (**Figure 3B**). On day 1, all cells exhibited round morphology with numerous dead cells along with live cells. On day 7, many elongated MSCs were observed, and far fewer dead cells were present. Lastly on day 15, most cells had elongated, and they were often seen

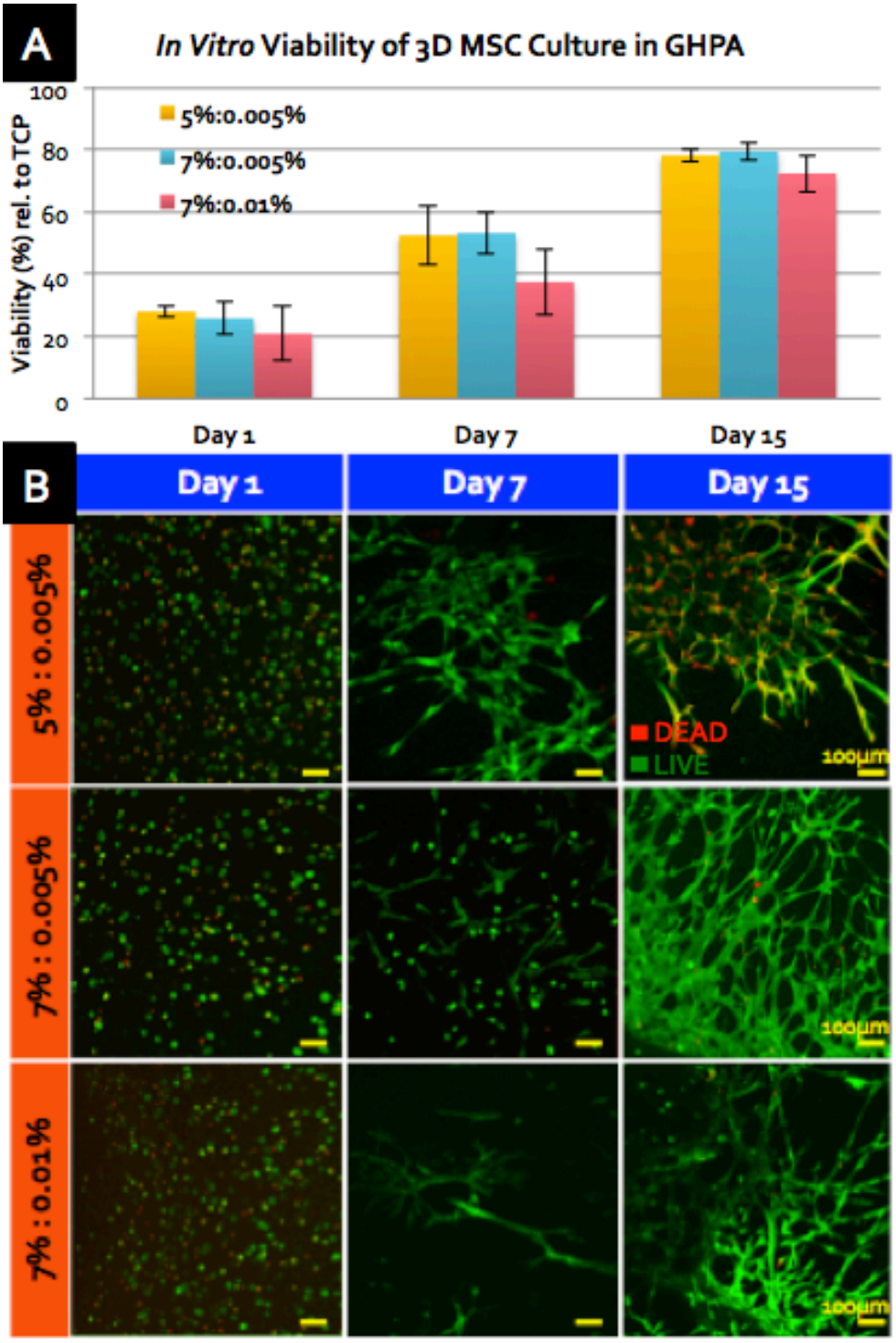

Figure 3. **(A)** *In vitro* cell viability of MSCs encapsulated in crosslinked GHPA gels on days 1, 7, and 15 compared to MSCs on tissue culture polystyrene (TCPS) by resazurin reduction with N=3 and error bars = ±1 SD. X%:Y% denotes X %w/v gelatin and Y %w/v H_2O_2. **(B)** Confocal images of Live/Dead staining of 3D MSC culture in GHPA on days 1, 7, and 15.

forming branched tube networks, while the top surface of GHPA gel was completely covered by a layer of MSCs (data not shown). Overall, crosslinked GHPA gels supported robust MSC proliferation within and on the surface, and the changes in cell morphology and organization showed active cell-material interactions towards vasculogenesis.

In Vitro MSC Differentiation to Endothelial Lineage in GHPA

Since the unusual organization of branching tube networks was observed in MSCs encapsulated in GHPA gels on day 15 (**Figure 3B**), we tested if this material promotes MSC differentiation to a certain lineage upon encapsulation *in vitro*. Again MSCs were encapsulated and cultured in GHPA gels for 15 days, and their RNA was collected. Initial differentiation survey was done by RT-PCR for myogenic (*MyoD*), cardiac (*GATA-4*), neural (*Nfl*), and endothelial (*Flk-1*) markers, and the PCR products were run on an agarose gel for visualization. Among the markers investigated, only *Flk-1* showed a positive expression (data not shown), hence we decided to further characterize potential MSC differentiation into an endothelial lineage by qRT-PCR for *CD31* and *Flk-1*, and the results are shown in **Figure 4A**. For both endothelial markers, MSCs grown in GHPA gels showed statistically significant up-regulation of *CD31* (>5 folds) and *Flk-1* (≈ 4 folds) expression in all GHPA conditions in comparison to MSCs on TCPS ($p < 0.05$).

To test if such increase in the *Flk-1* expression at the gene level was reflected at the protein level, we used *Flk-1-LacZ* transgenic murine MSCs. These cells were cultivated in an identical condition, and on day 15 LacZ expression was assayed at both the gene and protein levels where positive LacZ expression would imply positive expression for Flk-1 (**Figure 4B**). Interestingly, the MSCs cultured in 5%:0.005% condition were positive for LacZ expression at both the gene and protein levels. Of note, these transgenic cells were noticeably slower in growth and elongation while encapsulated in GHPA gels compared to the wild type MSC. In fact, it was evident from

cryosectioned samples that *Flk-1-LacZ* MSCs were mainly located near the surface, and fewer cells were observed throughout the gel, possibly indicating difficulties in surviving in GHPA gels for the transgenic cells. Hence it may require additional culture time for *Flk-1-LacZ* MSCs to reach the same extent of proliferation and differentiation in GHPA gels compared to the wild type MSCs.

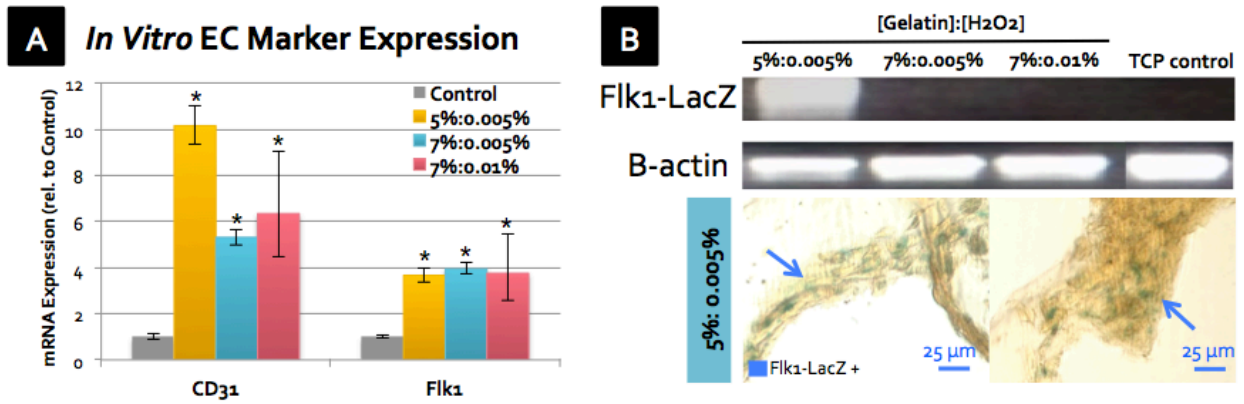

Figure 4. **(A)** MSC expression for endothelial cell markers *CD31* and *Flk-1* were determined from mRNA after 15 days of culture in GHPA gels by qRT-PCR with N=3 and error bars = ±1 SEM. * indicates $p<0.05$ in comparison to control MSCs on tissue culture plate. **(B)** *Flk1-LacZ* transgenic MSCs were cultured in GHPA gels for 15 days and assayed for *LacZ* mRNA expression by qRT-PCR and protein expression by β-galactosidase stain on day 15.

In Vivo Subcutaneous Implantation of MSC-containing GHPA Gels

In order to confirm the effect of GHPA gels on MSC differentiation towards the endothelial lineage *in vitro*, we investigated the potential pro-angiogenic effect of MSC-delivering GHPA gels *in vivo*. *Flk-1-LacZ* MSC-containing GHPA gel was injected into porous, non-biodegradable PVA sponges, and the gel-PVA sponge complexes were implanted into ventral subcutaneous regions in the wild type C57Bl/6 mice for 2 weeks (**Figure 5A**). Because multiple implantations are possible in each mouse, this model enabled better control in biological variability among the mice and better comparisons among the test conditions, and reduced the number of the animals required. Four different gel-PVA scaffolds were implanted in each mouse: a control containing MSCs in non-crosslinked GHPA and three gel-scaffolds carrying MSCs in different crosslinked GHPA gel formulations (5%:0.005%, 7%:0.005%, and 7%:0.01%). PVA scaffolds were necessary to track the

delivered cells and GHPA, as gelatin is known for fast *in vivo* degradation by host matrix metalloproteinase (MMPs) [12]. Similarly, *Flk-1-LacZ* transgenic MSCs were used to distinguish the implanted cells from host cells and provided a convenient reporter system where their phenotypic change into an endothelial lineage is indicated by positive LacZ expression.

After 2 weeks of implantation, the scaffolds were harvested and sectioned for various analyses. Trichrome green staining was used to visualize collagen/GHPA (green-light blue), cytoplasm of various cell types (purple-red), and erythrocytes (small pink rings due to their lack of nuclei) (**Figure 5B**). In all conditions, there was robust leukocyte infiltration indicated by extensive distribution of round purple-red cells slightly bigger than erythrocytes which are small pink rings throughout the scaffolds, and erythrocytes were often observed as well. However, there were two significant differences among the conditions: **1)** more collagen and/or gelatin was present in conditions with higher GHPA and hydrogen peroxide contents, and sometimes chunks of remaining GHPA with few cells were observed in crosslinked GHPA conditions (e.g., left side in the upper image for 7%:0.01% condition), and **2)** crosslinked GHPA conditions frequently exhibited vascular capillaries throughout the scaffolds with organized branches of cells extending few hundred microns that contained erythrocytes. However, such organization was largely lacking in the control. Additionally, it was evident that there was no giant foam cells or fibrous capsule formation around the chunks of crosslinked GHPA.

Sections were also stained for β-galactosidase activity to reveal Flk-1-LacZ positive MSCs that were implanted (**Figure 5C**). It is clear that all three crosslinked GHPA conditions retained many implanted MSCs that were positive for Flk-1-LacZ (blue) staining throughout the scaffolds , indicating MSC differentiation into an endothelial lineage *in vivo*. For the control condition, Flk-1-LacZ-positive MSCs were mostly observed near the surface of the PVA scaffolds, and far fewer in quantity.

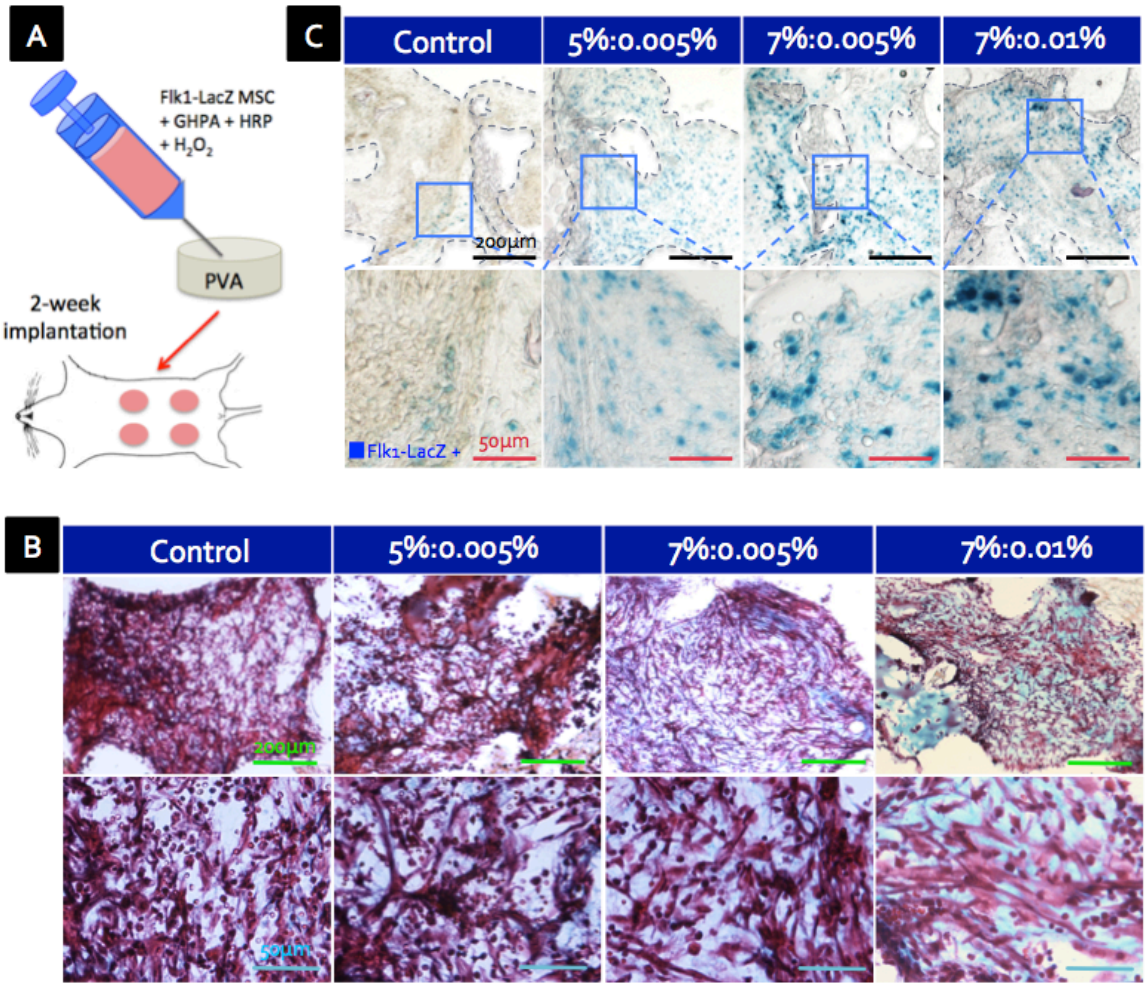

Figure 5. **(A)** Schematic of *In vivo* experiment where *Flk-1-LacZ* MSCs-containing GHPA was injected into and crosslinked within a porous PVA scaffold for a murine ventral subcutaneous implantation. **(B)** Trichrome green staining of cross-sections of scaffolds at 2 weeks post implantation where cytoplasm is stained red, erythrocytes pink and collagen/GHPA gels blue/green. **(C)** β-galactosidase staining shows that delivered *Flk-1-LacZ* MSCs were retained and became Flk1-LacZ+ post 2-week implantation in crosslinked GHPA conditions. The boxes indicate Flk1-LacZ+ cell-containing areas. **(B-C)** Upper images with a scale bar = 200μm, and lower images with a scale bar = 50μm.

In Vivo Pro-Angiogenic Effect of MSC Delivery in GHPA

In order to visualize the functional neovasculature in the implanted PVA scaffolds, mice were perfused with saline containing fluorescent microbeads for micro-angiography before harvesting the scaffolds. The resulting micro-angiograms from the surface and cross-sections of the scaffolds for each condition are shown in the upper panel of **Figure 6**. Note that all angiograms

shown are from the same mouse. Neovasculature in implanted scaffolds are different from the vasculature in the native host tissues around the implantation site in two important ways: 1) implanted scaffolds are not as profusely vascularized as the ones surrounding the host tissues, and 2) neovasculature in/on scaffolds are mostly tortuous and branching in shape while the vasculature in the neighboring tissues exhibits well-organized blood vessels running straight and parallel to each other (data not shown). Across all conditions, the surfaces of the implanted scaffolds showed well-connected and well-developed functional vasculature where smaller capillaries with diameters < 10μm sprouted from larger arterioles that were 20-30μm in diameters. The control scaffold also formed a considerable amount of neovasculature on its surface. However, the crosslinked GHPA conditions especially in the 7%:0.01% condition showed a drastic enhancement in angiogenesis on the surface compared to the control.. On the other hand, the micro-angiograms from the cross-sections of the scaffolds reveal an even more stark difference between the control and crosslinked GHPA conditions, where the control condition showed a limited degree of neovasculature at the perimeter of the scaffold while the crosslinked GHPA gels supported robust angiogenesis throughout the cross-sections. Understandably, there is a lesser amount of vasculature seen on the cross-sections than on the surfaces due to limited access, and blood vessels exhibited even more tortuosity within the scaffold likely due to the physical obstacles in the form of non-biodegradable PVA scaffold.

Blood vessel formation was further confirmed by CD31 staining of the cross-sections of the scaffolds as shown in the bottom panel of **Figure 6**. In all conditions, there were two types of CD31+ cells. The first type was individual cells with a circular nucleus and CD31 expression around the nuclei, likely indicating infiltrating leukocytes [13], and the second type exhibited elongated nuclei and CD31 expression with tubular structures spanning ~50μm, indicating blood vessels. CD31 staining of the control section is in agreement with the micro-angiogram where the vasculature is mostly formed near the surface (the right side of the image), with few CD31+ infiltrating single

cells. In contrast, all three crosslinked GHPA conditions showed numerous CD31+ cells both as single cells and in tubular structures, indicative of blood vessels. In 5%:0.005% and 7%:0.01% conditions, capillaries about 10μm in diameter were dominant while the 7%:0.005% condition also exhibited newly forming tubes with diameters in the 4~5μm range. Taken together, the angiograms and CD31 staining showed functional, perfusable neovasculature formation throughout the implanted scaffolds for crosslinked GHPA conditions, while only a limited degree of vascularization was seen near the surface for the control scaffolds.

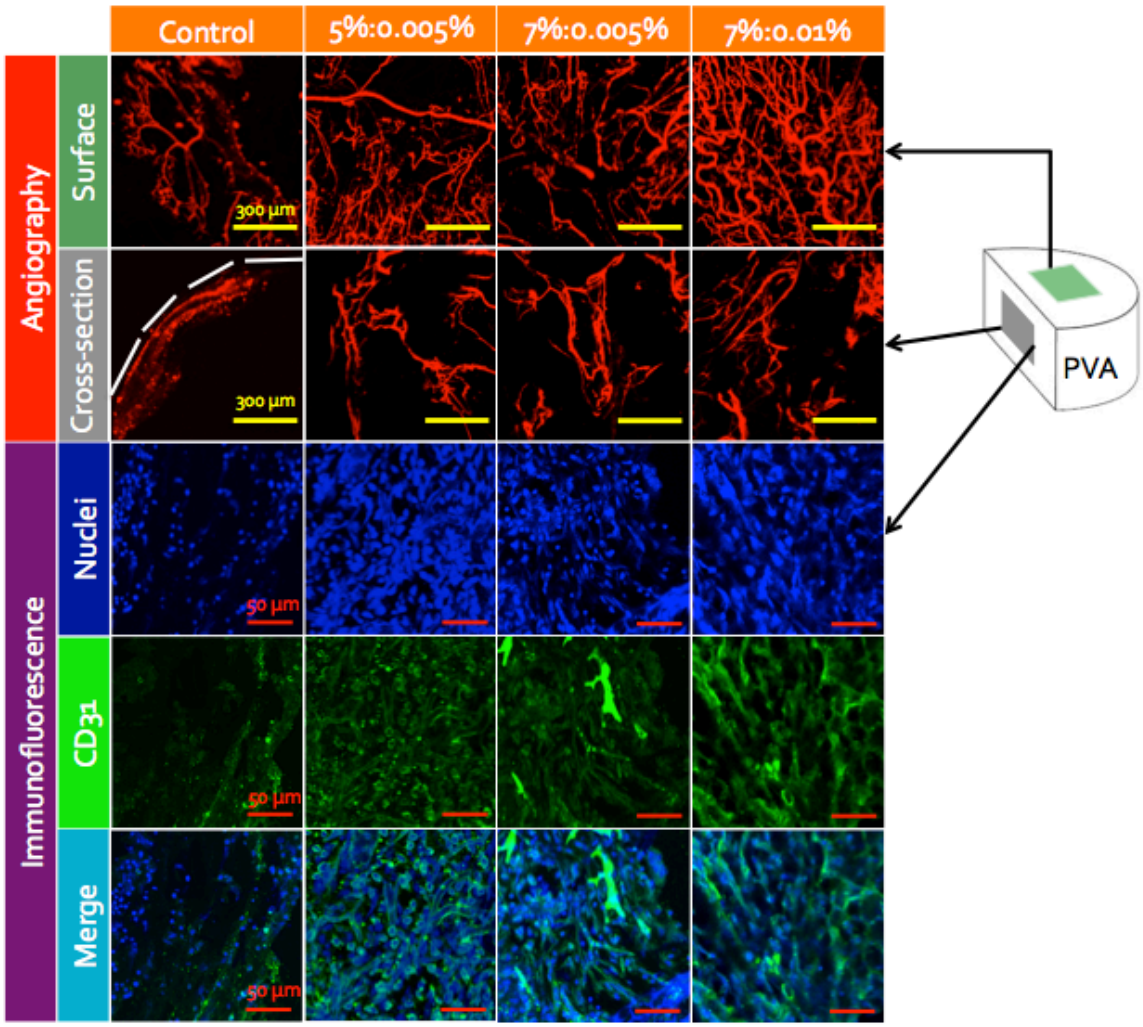

Figure 6. Upper panel shows micro-angiograms from the scaffolds at 2 weeks post implantation acquired by perfusing mice with fluorescent beads. Representative images from the outer surface and cross-sections are shown. White dotted line marks the boundary of the scaffold. Bottom panel shows CD31 and nuclei stained cross-sections of explanted scaffolds. All images were acquired by confocal microscopy.

In Vivo Gene Expression in GHPA Gels Delivering MSCs

RNA collected from the harvested scaffolds was analyzed by qRT-PCR to quantitatively analyze gene expression. Both the early (*Flk-1, VE-cadherin, CD31*) and mature stage markers (*vWF*) of angiogenesis were analyzed, and the results are shown in **Figure 7A**. Angiogenesis markers, especially those for the early stage, were significantly up-regulated in the crosslinked GHPA conditions compared to the control. For Flk-1, crosslinked GHPA conditions showed approximately 1-, 2-, 3-fold increases in expression for 5%:0.005%, 7%:0.005%, and 7%:0.01% respectively. For *VE-cadherin*, crosslinked GHPA conditions showed approximately 1-, 4-, and 12-fold increases in expression for 5%:0.005%, 7%:0.005%, and 7%:0.01% respectively. In a similar trend, CD31 expression showed 1-, 1-, and 3-fold increases for 5%:0.005%, 7%:0.005%, and 7%:0.01%, respectively. For these early angiogenesis markers (*Flk-1, VE-cadherin* and *CD31*), there was a clear positive correlation between the marker expression and the GHPA content/crosslinking degree. However, this trend was not observed for the late stage angiogenesis marker, *vWF*, where all crosslinked GHPA conditions had about 60% increase in comparison to the control condition. This may be due to the fact that vWF expression varies depending on the organ and blood vessel type, and is rarely observed in small capillaries or neovasculature [14]. Collectively, these results demonstrate that overall there were significant increases in angiogenesis in crosslinked GHPA conditions, and that such increases were even more pronounced in conditions with higher amounts of GHPA and crosslinking.

We also measured the expression of two markers (*iNOS* and *MRC1*) that represent the host macrophage response to the implants (**Figure 7B**). Both *iNOS* and *MRC1* are macrophage-specific markers with iNOS expression associated with a classically-activated/inflammatory macrophage phenotype while MRC1 expression is closely associated with an alternatively-activated/reparative macrophage phenotype [15]. For iNOS expression, the 5%:0.005% showed a 50% increase compared to the control, however, iNOS expression for 7%:0.005% was about the same, and 7%:0.01%

showed a 50% decrease in comparison to the control. For MRC1, there was again the GHPA/crosslinking-dependent trend of increasing expression with 7%:0.01% condition having the highest level of MRC1 expression at 1.9-fold that of the control. These results indicate that the 7%:0.01% condition invoked a favorable response from the host macrophages with reduced iNOS expression and increased MRC1 expression.

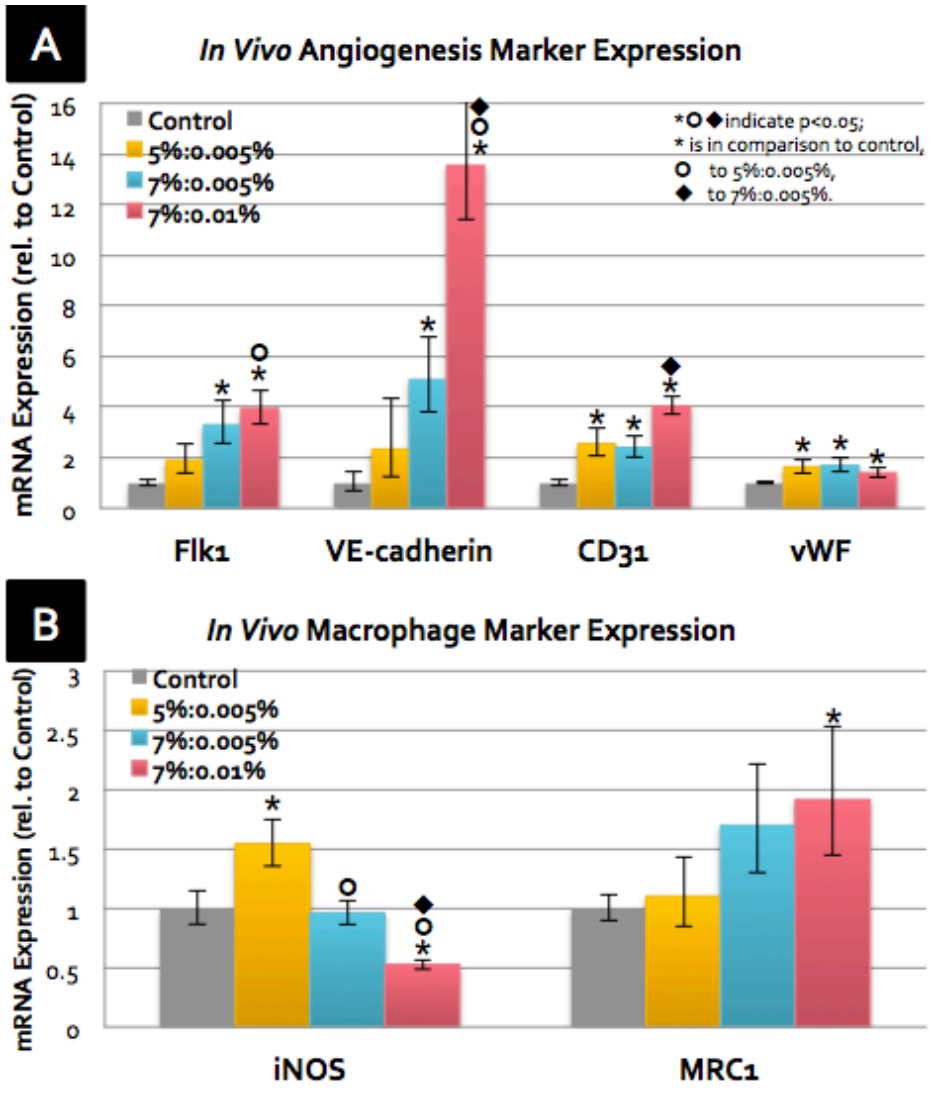

Figure 7. 2 weeks post implantation, explanted scaffolds were assayed for gene expression **of (A)** angiogenesis/ endothelial cell markers and **(B)** macrophage markers by qRT-PCR with N=4 and error bars = ±1 SEM.

Table 1. List of primers.

Genes	Forward Primer	Reverse Primer
β-Actin	TCGTGCGTGACATCAAAGAG	TGGACAGTGAGGCCAGGATG
CD31	TCCCTGGGAGGTCGTCCAT	GAACAAGGCAGCGGGGTTTA
Flk-1	GAGAGCAAGGCGCTGCTAGC	GACAGAGGCGATGAATGGTG
GAPDH	TGAAGCAGGCATCTGAGGG	CGAAGGTGGAAGAGTGGGAG
iNOS	CCAAGCCCTCACCTACTTCC	CTCTGAGGGCTGACACAAGG
LacZ	GCGTTAACTCGGCGTTTCAT	GCGCTCAGGTCAAATTCAGAC
MRC-1	TTGTGGTGAGCTGAAAGGTG	GTGGATTGTCTTGTGG
VE-cadherin	TCCTCTGCATCCTCACTATCACA	GTAAGTGACCAACTGCTCGTGAAT
vWF	GCTTGAACTGTTTGACGGAGAGG	TGACCCAGCAGCAGGATGAC

Discussion

The primary purpose of this study was to evaluate *in situ* crosslinkable gelatin as an advanced biomaterial template to promote vasculogenesis when used to deliver MSCs. With wide availability, economic production, excellent biocompatibility, and non-antigenicity, gelatin is worth serious consideration as a highly functional biomaterial. However, its use has been severely limited due to its low upper critical solution temperature below 35°C [6]. Conjugation of hydroxyphenyl propionic acid to the gelatin backbone enables rapid H_2O_2- and horseradish peroxide (HRP)-mediated crosslinking, and such modification allows the use of gelatin as a thermo-stable hydrogel for biomedical applications at the body temperature of 37°C. As expected, crosslinked GHPA gels exhibited storage moduli (G') typical of soft hydrogels, and all test conditions gelled rapidly under 20 seconds at 37°C. Its rapid gelation property and injectability with relatively non-harsh crosslinking conditions make GHPA an excellent biomaterial platform for minimally invasive biomedical applications.

As a collagen-derived material, gelatin possesses numerous cell binding recognition sites with the RGD sequence being the most well-known and prevalent site [16]. This is a crucial advantage of collagen- or gelatin-based materials over synthetic ones (ie. Poly(ethylene glycol) hydrogels) whose cell attachment and viability are often insufficient [17] [18]. Most anchorage-dependent cells require attachment and spreading on a culture substrate for survival and proliferation, while poor

cell attachment with rounded morphology commonly results in reduced viability [19]. Accordingly, GHPA readily supported MSC cell attachment likely through the RGD binding, and most MSCs underwent clear cell spreading by day 15. Therefore, it is possible that this high level of cell attachment and spreading in crosslinked GHPA gels readily supported MSC proliferation.

Most interesting results from the initial measurement of cell viability of MSCs were the changes in cell network organization over time. At day 15, MSCs organized themselves into tubular networks that are typically seen with healthy endothelial cells on angiogenic substrates such as Matrigel. qRT-PCR results revealed that endothelial cell markers (CD31 and Flk-1) were indeed significantly up-regulated on day 15, and MSC differentiation towards the endothelial lineage was further confirmed by LacZ expression in *Flk-1-LacZ* transgenic MSCs. Many studies have previously shown MSC differentiation into endothelial cells *in vitro* using soluble factors such as VEGF and/or bFGF as well as *in vivo* [1a] [20] [21]. However, to our knowledge, this is the first reporting of MSC differentiation into an endothelial lineage purely by material effects without the use of soluble growth factors. Existing literature shows that cell-binding to the RGD sequence on gelatin or denatured collagen involves the activation of integrin αvβ3, which coincidentally is a crucial element in proliferation and migration/tubulogenesis of endothelial cells through its interactions with Flk-1 [16] [22]. In fact, blocking of αvβ3 is an effective way to restrict angiogenesis, and is investigated as an anti-cancer therapy, thus signifying the necessity and importance of αvβ3 in angiogenesis [23]. Hence, it is possible that MSCs on our crosslinked GHPA gels are up-regulating αvβ3 expression and activation through the RGD binding, and the activated αvβ3 then interacts with Flk-1 that was up-regulated by an unknown mechanism. Considering the fact that the cross-talk and interactions between αvβ3 and Flk-1 are required to initiate the signaling cascade for proliferation and capillary formation of endothelial cells, a similar mechanism may be responsible for MSC differentiation and tubulogenesis as observed in this study [22] [24]. However, further

investigation is needed to elucidate the exact mechanism of inducing endothelial differentiation from MSCs by crosslinked GHPA gels.

The pro-angiogenic effect of crosslinked GHPA gels was also shown *in vivo*. A multitude of assays was employed to confirm that when crosslinked GHPA gels delivered *Flk-1-LacZ* MSCs in porous, non-biodegradable PVA scaffolds, functional angiogenesis was markedly promoted throughout the scaffolds after 2 weeks of subcutaneous implantation, while the control condition with non-crosslinked GHPA had a limited degree of functional vascularization near the surface of the scaffold. Interestingly, there also appeared to be a positive correlation between the amount of neovasculature and the degree of GHPA content and crosslinking. This implies that the prolonged sustenance of GHPA gels *in vivo* may be a crucial factor in improving angiogenesis, as uncrosslinked gelatin is known to degrade rapidly *in vivo* by proteases such as matrix metalloproteinases (MMPs), and there was significantly less angiogenesis [12]. Therefore, without crosslinking the tubulogenic effect we observed in *in vitro* experiments was lost in the control condition, while the condition containing the most GHPA with the highest level of crosslinking showed the highest degree of angiogenesis.

Only a very small number of studies investigated angiogenesis in thermally and chemically crosslinked gelatin implants using Gelfoam® that is commercially and clinically available. These studies showed significant angiogenesis in the implants when implanted alone [25] [26]. Interestingly, it was also shown that crosslinked gelatin scaffolds promoted angiogenesis significantly better than similarly prepared collagen scaffolds [25]. Our study is also in support of the *in vivo* pro-angiogenic effect of crosslinked gelatin, however, our results are convoluted by the use of MSCs. Therefore, the angiogenic effect of crosslinked gelatin material alone and especially comparisons to other materials need to be investigated further.

Another important advantage of gelatin material is its non-immuno/antigenicity *in vivo*, as the harsh gelatin extraction process is thought to remove known antigens existing on intact 3D

collagen [27]. Injections of unmodified gelatin into several animals also failed to produce antibodies [28]. On the other hand, the abovementioned studies involving crosslinked gelatin sponges reported negligible inflammation and no scarring/fibrous capsule formation when implanted [29] [25] [26]. We also observed no giant foam cells or dense collagen deposition around the implanted GHPA gels. Furthermore, the gene expression profile revealed a significant increase in reparative macrophage recruitment, while there was a reduction in inflammatory macrophages in the highest GHPA content condition with the most crosslinking. Hence, the conjugation of hydroxyphenyl propionic acid to gelatin likely retains the non-immuno/antigenicity of the unmodified gelatin, and highly crosslinked GHPA gel further invoked favorable interactions with host macrophages, which can forecast better long-term integration with the host tissues.

CHAPTER III

CONCLUSION

In this study, we have synthesized an injectable and *in situ* crosslinkable gelatin-based biomaterial that was highly biocompatible and showed a marked pro-angiogenic effect by promoting endothelial differentiation of MSCs both *in vitro* and *in vivo*. Crosslinked GHPA gels resulted in robust formation of neovasculature throughout the implants in coordination with non-immuno/antigenicity and favorable macrophage responses. Of note, this is the first time to report that a material can induce MSC differentiation into an endothelial lineage without the use of soluble growth factors. The results are also highly significant as this is the first study to use a purely gelatin-based material in a form of injectable hydrogel for vasculogenic delivery of stem cells in the fields of tissue engineering and regenerative medicine, which has been largely impossible previously. Because of the short history of using gelatin-based materials in tissue engineering applications, the exact mechanisms for improved angiogenesis by crosslinked gelatin and 3D gelatin-cell interactions remain to be elucidated. Further studies are needed to better understand the apparent and numerous advantages of GHPA and its optimal applications in specific biomedical fields.

REFERENCES

1. Werner, R., Mechanisms of angiogenesis. *Nature* **1997,** *386* (17), 671-674.
2. Rouwkema, J.; Rivron, N. C.; van Blitterswijk, C. A., Vascularization in tissue engineering. *Trends in biotechnology* **2008,** *26* (8), 434-41.
3. Lovett, M.; Kaplan, D. L., Vascularization strategies for tissue engineering. *Tissue Engineering: Part B* **2009,** *15* (3), 353-376.
4. Gorgieva, S.; Kokol, V., Collagen- vs. gelatin-based biomaterials and their biocompatibility: review and perspectives. In *Biomaterials Applications for Nanomedicine*, R, P., Ed. InTech: 2011; pp 17-52.
5. Flkman, J.; Zetter, B. R., Long-term culture of capillary endothelial cells. *Proc. Natl. Acad. Sci. USA* **1979,** *76* (10), 5217-5221.
6. Bohidar, H. B.; Gupta, A., Flory temperature and upper critical solution temperature of gelatin solutions. *Biomacromolecules* **2005,** *6*, 1623-1627.
7. Lee, Y.; Bae, J. W.; Oh, D. H.; Park, K. M.; Chun, Y. W.; Sung, H.-J.; Park, K. D., In situ forming gelatin-based tissue adhesives and their phenolic content-driven properties. *Journal of Materials Chemistry B* **2013,** *1* (18), 2407.
8. Minguell, J. J.; Congel, P., Mesenchymal Stem Cells. *Exp Biol Med* **2001,** *226*, 507-520.
9. Uccelli, A.; Moretta, L.; Pistoia, V., Mesenchymal stem cells in health and disease. *Nature reviews. Immunology* **2008,** *8* (9), 726-36.
10. Caplan, A. I.; Correa, D., The MSC: an injury drugstore. *Cell stem cell* **2011,** *9* (1), 11-5.
11. Willems, E.; Leyns, L.; Vandesompele, J., Standardization of real-time PCR gene expression data from independent biological replicates. *Analytical biochemistry* **2008,** *379* (1), 127-9.
12. Agren, M. S., Gelatinase activity during wound healing. *British Journal of Dermatology* **1994,** *131*, 634-640.
13. Duncan, G. S.; Mak, T. W., Genetic evidence for functional redundancy of platelet/endothelial cell adhesion molecule-1 (PECAM-1): CD31-deficient mice reveal PECAM-1-dependent and PECAM-1-independent functions. *Journal of immunology* **1999,** *162*, 3022-3030.
14. Van Amerongen, M. J.; Van Luyn, M. J. A., Neovascularization and vascular markers in a foreign body reaction to subcutaneously implanted degradable biomaterial in mice. *Angiogenesis* **2002,** *5*, 173-180.
15. Sica, A.; Mantovani, A., Macrophage plasticity and polarization: in vivo veritas. *The Journal of clinical investigation* **2012,** *122* (3), 787-95.
16. Davis, G. E., Affinity of integrins for damaged extracellular matrix: avb3 binds to denatured collagen type I trhough RGD sites. *Biochemical and biophysical research communications* **1992,** *182* (3), 1025-1031.
17. Benoit, D. S.; Durney, A. R.; Anseth, K. S., The effect of heparin-functionalized PEG hydrogels on three-dimensional human mesenchymal stem cell osteogenic differentiation. *Biomaterials* **2007,** *28* (1), 66-77.

18. Hern, D. L.; Hubbell, J. A., Incorporation of adhesion peptides into nonadhesive hydrogels useful for tissue engineering. *Journal of biomedical materials research. Part B, Applied biomaterials* **1997,** *39* (2), 266-276.
19. Ingber, D. E., Fibronectin controls capillary endothelial cell growth by modulating cell shape. *Proc. Natl. Acad. Sci. USA* **1990,** *87*, 3579-3583.
20. Cao, Y.; Sun, Z.; Liao, L.; Meng, Y.; Han, Q.; Zhao, R. C., Human adipose tissue-derived stem cells differentiate into endothelial cells in vitro and improve postnatal neovascularization in vivo. *Biochemical and biophysical research communications* **2005,** *332* (2), 370-9.
21. Silva, G. V.; Litovsky, S.; Assad, J. A.; Sousa, A. L.; Martin, B. J.; Vela, D.; Coulter, S. C.; Lin, J.; Ober, J.; Vaughn, W. K.; Branco, R. V.; Oliveira, E. M.; He, R.; Geng, Y. J.; Willerson, J. T.; Perin, E. C., Mesenchymal stem cells differentiate into an endothelial phenotype, enhance vascular density, and improve heart function in a canine chronic ischemia model. *Circulation* **2005,** *111* (2), 150-6.
22. Brooks, P. C.; Clark, R. A. F.; Cheresh, D. A., Requirement of Vasculra Integrin alpha v beta 3 for angiogenesis. *Science* **1994,** *264* (5158), 569-571.
23. Ruegg, C.; Alghisi, G. C., Vascular integrins: therapeutic and imaging targets of tumor angiogenesis. In *Angiogenesis Inhibition*, P.M., S.; H.J., S., Eds. Springer: 2010.
24. Somanath, P. R.; Malinin, N. L.; Byzova, T. V., Cooperation between integrin alphavbeta3 and VEGFR2 in angiogenesis. *Angiogenesis* **2009,** *12* (2), 177-85.
25. Dreesmann, L.; Ahlers, M.; Schlosshauer, B., The pro-angiogenic characteristics of a cross-linked gelatin matrix. *Biomaterials* **2007,** *28* (36), 5536-43.
26. Ribatti, D.; Nico, B.; Vacca, A.; Presta, M., The gelatin sponge-chorioallantoic membrane assay. *Nature protocols* **2006,** *1* (1), 85-91.
27. Lynn, A. K.; Yannas, I. V.; Bonfield, W., Antigenicity and immunogenicity of collagen. *Journal of biomedical materials research. Part B, Applied biomaterials* **2004,** *71* (2), 343-54.
28. Starin, W. A., The antigenic properties of gelatin. *the journal of infectious diseases* **1918,** *23* (2), 139-158.
29. Ponticiello, M. S.; Barry, F. P., Gelatin-based resorbable sponge as a carrier matrix for human mesenchymal stem cells in cartilage regeneration therapy. *Journal of biomedical materials research. Part B, Applied biomaterials* **2000,** *52* (2), 246-255.